Received: 11 January 2022 | Revised: 29 March 2022 | Accepted: 11 April 2022

DOI: 10.1111/jace.18510

Journal of American Ceramic Society

RESEARCH ARTICLE

Microstructure evolution in Si^+ ion irradiated and annealed Ti_3SiC_2 MAX phase

Chao Ye[1] | **Qing Chang**[1] | **Penghui Lei**[2] | **Wenhui Dong**[1] | **Qing Peng**[3]

[1]Yangtze River Delta Research Institute, Northwestern Polytechnical University, Xi'an, China

[2]School of Nuclear Science and Technology, Xi'an Jiaotong University, Xi'an, China

[3]State Key Laboratory of Nonlinear Mechanics, Institute of Mechanics, Chinese Academy of Sciences, Beijing, China

Correspondence
Chao Ye, Northwestern Polytechnical University, Xi'an 710072, China.
Email: yechao@nwpu.edu.cn

Qing Peng, State Key Laboratory of Nonlinear Mechanics, Institute of Mechanics, Chinese Academy of Sciences, Beijing 100190, China.
Email: PengQing@imech.ac.cn

Funding information
NPL, CAEP, Grant/Award Number: 2015AB001; National major scientific research equipment development of China, through, Grant/Award Number: 11227804; Chinese Academy of Sciences through, Grant/Award Number: E1Z1011001

Abstract

Ti_3SiC_2 samples were irradiated by a 6-MeV Si^+ ion to a fluence of 2×10^{16} Si^+ ions/cm^2 at 300°C followed by annealing at 900°C for 5 h. A transmission electron microscope was used to characterize microstructural evolution. The phase of Ti_3SiC_2 transformed from the hexagonal close-packed (HCP) to a face-centered cubic structure after irradiation. Hexagonal screw dislocation networks were identified at the deepest position of the irradiated area, which are the products of dislocations reactions. After annealing, the irradiated region has reverted to the original HCP structure. High-density cavities and stacking faults were formed along the basal planes. In addition, ripplocations have been observed in the irradiated region in the Ti_3SiC_2 sample after annealing. Our insights into the formation processes and corresponding mechanisms of these defect structures might be helpful in the material design of advanced irradiation tolerance materials.

KEYWORDS

annealing, dislocation networks, ion irradiation, ripplocations, Ti_3SiC_2

1 | INTRODUCTION

In recent years, a class of ternary layered hexagonal carbides and nitrides called MAX phases have attracted extensive research attention.[1,2] MAX phases have the general chemical formula of $M_{n+1}AX_n$, where $n = 1$–3 and M is an early transition metal element (such as Ti, V, and Nb), A is an A-group element (such as Al and Si) and X is either C and/or N.[3–6] The unique crystal structure and electronic density of states make MAX phase materials exhibit both ceramic and metallic properties: low density, perfect heat conductivity, high strength, excellent corrosion resistance, and high-temperature oxidation resistance.[7] Fracture energy absorption mechanisms, such as crack deflection, interlaminar tearing, and inter-grain slippage, make the MAX phase have good plastic deformation behavior.[8] Due to their remarkable properties, MAX phase materials have been used in various applications, such as MAX phase material heaters, three-way crystal reactors, gas burner nozzles, Ta_2AlC/Ag bearing and superalloy foils, and two-dimensional layered MXene material for batteries.[9] So far, roughly 155 different types of MAX phases have been discovered/synthesized.[10] The chemical diversity and highly resistance to radiation damage make many MAX

phases the promising candidate materials for nuclear reactors,[11–14] wherein the materials are exposed to a harsh service environment: high radiation, high temperature, and highly corrosive environment.

It has been found that $M_{n+1}AX_n$ phases experienced mechanical property changes and phase transformations under radiation conditions.[15,16] Mental et al.[17,18] showed that the specific activities of Ti_3SiC_2 and Ti_2AlC MAX phases were similar to SiC materials under 60-year thermal neutron and fast neutron irradiations. Moreover, they are three orders of magnitude lower than that of Alloy 617 nickel-based alloy, which makes the MAX phases a potential coating material to protect the Zircaloy tubes. Besides, Filbert[19] and Spencer[20] verified that the Ti_3SiC_2 MAX phase, which has good chemical compatibility with SiC, could be used as a nuclear-used SiC_f/SiC composite interphase coating material. Under neutron irradiation, the evolution of microstructures of MAX phases with different chemistry is very complex. For example,[21] with the increase of radiation damage from 2 to 10 dpa, the cavities were seen to form only along grain boundaries (GBs) in Ti_3SiC_2. However, they were seen to be well dispersed in the matrix of the Ti_2AlC. Some neutron radiation results suggest that Ti_3SiC_2 could be used at temperatures higher than 700°C in reactors as the volume fraction of TiC and densities of stacking faults (SFs) are eliminated or minimized under such condition.[22] The electrical and thermodynamic resistivities of several MAX phases, including Ti_3AlC_2, Ti_3SiC_2, Ti_2AlC, and Ti_2AlN, were found to increase with the fluence under neutron irradiation as the density of radiation-induced point defects that can scatter charge carrier increases.[16]

There are also many studies on the behaviors of the MAX phases under ion irradiation, which showed most MAX phases have superior ion irradiation resistance.[23] For example, Ti_3AlC_2 was found to be amorphous-resistant up to 52 and 25 dpa under irradiation by 500-keV He ions and 1-MeV Xe ions, respectively.[24,25] However, the Cr-containing MAX phases, such as Cr_2AlC and Cr_2GeC, show poor radiation resistance.[26] In addition, the irradiation-induced expansion of crystal lattices of MAX phases could lead to microstrain and volumetric swelling resulting in cracking.[27] Anisotropic lattice changes were seen in Ti_3AlC_2 and Ti_3SiC_2 MAX phases resulting in cracking along GBs under heavy ion irradiation at temperatures below 400°C.[28] Under light ion irradiation like helium ion irradiation, Ti_3SiC_2 was found to have an excellent He impurities resistance and could retain its mechanical properties under the high-temperature irradiation conditions.[29]

Compared with the complex microstructure evolutions caused by the synergistic effects of neutron irradiation, ion irradiation can specifically study the influence of a specific irradiation factor on the structure of the material. For example, heavy ion irradiation mainly studies the influence of radiation damage on materials, whereas light ion irradiation mainly studies the influence of transmutation products on materials. Meanwhile, some specific heavy ions can simulate specific fission product elements in the reactor. Thus, in order to study the effects of radiation damage and annealing process on the microstructure of the Ti_3SiC_2 material, in the present study, Si ion was injected into the Ti_3SiC_2 bulk sample at 300°C then annealed the sample at 900°C. The formation processes and corresponding mechanisms of different defects that caused by radiation damage are discussed in detail in the following section.

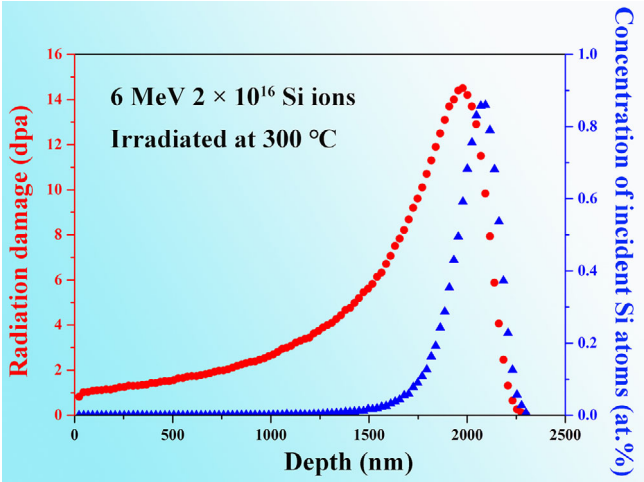

FIGURE 1 The distribution of radiation damage and concentration of incident Si atoms with respect to the depth of silicon ion–irradiated Ti_3SiC_2 from the simulation by SRIM-2013 software. SRIM, Stopping and Range of Ions in Matter

2 | EXPERIMENTS

Commercial Ti_3SiC_2 bulk materials were irradiated by Si^+ ions at an energy of 6 MeV up to a fluence of 2×10^{16} Si^+ ions/cm^2 at 300°C. The materials were then annealed in an argon (99.999% purity) protection tube furnace at 900°C for 5 h. To estimate the damage level, Stopping and Range of Ions in Matter (SRIM) software with full damage cascades mode was employed with the displacement threshold energies of Ti, Si, and C atoms in Ti_3SiC_2 being set as 25, 15, and 28 eV,[30] respectively. And the material density of Ti_3SiC_2 in the calculations was set as 4.52 g/cm^3.[31] The calculated depth variation of radiation damage and incident Si concentration are shown in Figure 1A. At the 2×10^{16} Si^+ ions/cm^2 fluence, the damage level is 14.5 dpa. In order to avoid the influence of impurity elements on the microstructure and composition

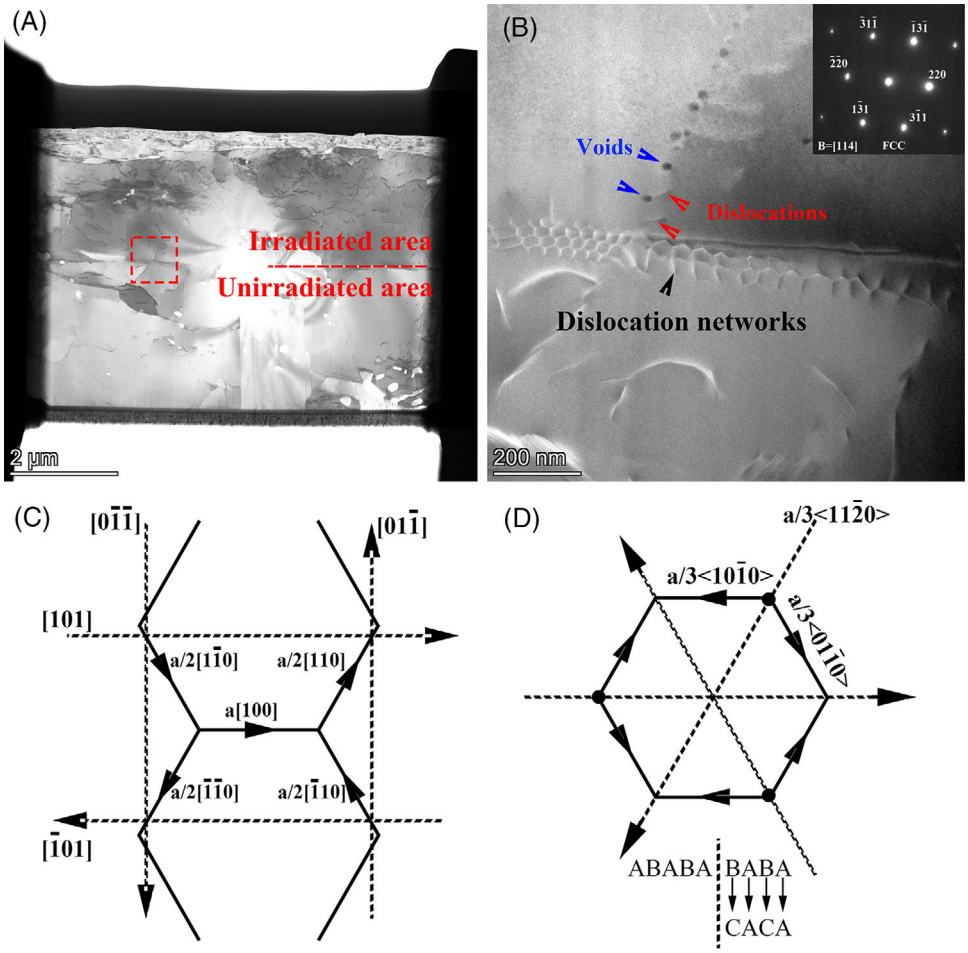

FIGURE 2 (A) A cross-sectional STEM BF image of the Si^+ ion–irradiated Ti_3SiC_2 sample; (B) a magnified STEM DF image of the red frame region in (A) and the inset is an SAED pattern from the irradiated Ti_3SiC_2 region; (C) and (D) schematic diagrams of the HSDNs in FCC- and HCP-structured materials, respectively. BF, bright-field; DF, dark-field; FCC, face-centered cubic; HCP, hexagonal close-packed; HSDNs, hexagonal screw dislocation networks; SAED, selected area electron diffraction

of the Ti_3SiC_2 material after irradiation, Si^+ ions were used for the irradiation experiment.

An FEI-Talos FX200 TEM was used for characterizing the microstructures of the materials. Selected area electron diffraction (SAED) patterns and element maps by energy-dispersive spectroscopy (EDS) as well as high-resolution TEM (HRTEM) images were collected from the materials. The specimens for TEM study were prepared by using a focused ion beam method with the thickness less than 100 nm.

3 | RESULTS AND DISCUSSION

Figure 2A is a cross-sectional STEM bright-field image showing the irradiated (in the top) and unirradiated regions (in the bottom) with their boundary marked by a horizontal dotted line. Compared with the unirradiated region, there are more dislocations in the irradiated region, indicating the formation and accumulation of interstitial defects under the 6 MeV Si^+ ion irradiation at 300°C. Figure 2B is a magnified STEM dark-field image of the region highlighted by a red dotted square frame. The SAED pattern taken from the irradiated region in Figure 2B indicates that the hexagonal close-packed (HCP) Ti_3SiC_2 phase has been transformed into a face-centered cubic (FCC) structure after irradiation. Ion irradiation–induced HCP-to-γ-to-FCC phase transformations have already been reported in many kinds of MAX phases, such as Ti_3AlC_2, V_2AlC, and Ti_4AlN_3.[15] Another feature that can be seen is that hexagonal screw dislocation networks (HSDNs) are formed at the interface region between the irradiated region with an FCC structure and the unirradiated region with an HCP structure. This means that the ion irradiation has induced the phase transformation of Ti_3SiC_2 from HCP to FCC structure and the formation of the HSDNs. The HSDNs have been observed in both pristine Ti_3SiC_2[21] and Ti_3AlC_2[23] phases with HCP structures and FCC

metals during high-temperature creep processes.[32,33] It has been generally agreed that the formation of the HSDNs is resulted from dislocation reactions. In a material with an FCC structure, four groups of dislocations of the hexagonal dislocation networks can be formed through Equations (1–4), as illustrated in Figure 2C.[32–34] The edge-type dislocation with the [1 0 0] burgers vector can be determined by Equation (5). The geometric condition of dislocation reaction Equation (5) is satisfied, but the energy condition is not. However, the irradiation-induced swelling can cause internal mechanical stresses, thus promoting the dislocation reaction.[35] And this kind of [1 0 0] segment dislocation had already been observed in Ni-based single-crystal superalloy.[32] Thus, such hexagonal dislocation networks near the damage peak region in the FCC–$(Ti_3Si)C_2$ crystal grain formed by the MAX phase transition during the ion irradiation process might be the product of dislocation reactions. In HCP-structured MAX phases, the perfect dislocation decomposition reactions can generate the SFs, as shown by Equation (6).[36] Thus, the formation mechanism of this kind of ordered hexagonal dislocation networks in the pristine Ti_3SiC_2 is due to the formation of Schottky partial dislocations generated by the decomposition reaction of perfect dislocations, as illustrated in Figure 2D.[32–34] Additionally, the SFs formed by the dissociation reaction (6) can trigger phase transformation from γ-$(M_{n+1}A)X_n$ to fcc-$(M_{n+1}A)X_n$[15,16]:

$$\frac{a}{2}[0\,1\,1] + \frac{a}{2}[1\,0\,\bar{1}] \rightarrow \frac{a}{2}[1\,1\,0] \tag{1}$$

$$\frac{a}{2}[0\,1\,1] + \frac{a}{2}[\bar{1}\,0\,\bar{1}] \rightarrow \frac{a}{2}[\bar{1}\,1\,0] \tag{2}$$

$$\frac{a}{2}[0\,1\,\bar{1}] + \frac{a}{2}[\bar{1}\,0\,1] \rightarrow \frac{a}{2}[\bar{1}\,1\,0] \tag{3}$$

$$\frac{a}{2}[0\,1\,\bar{1}] + \frac{a}{2}[1\,0\,1] \rightarrow \frac{a}{2}[1\,1\,0] \tag{4}$$

$$\frac{a}{2}[1\,0\,1] + \frac{a}{2}[1\,0\,\bar{1}] \rightarrow a[1\,0\,0] \tag{5}$$

$$\frac{1}{3}\langle 1\,1\,\bar{2}\,0\rangle \rightarrow \frac{1}{3}\langle 1\,0\,\bar{1}\,0\rangle + \text{stacking faults} + \frac{1}{3}\langle 0\,1\,\bar{1}\,0\rangle \tag{6}$$

In the Si^+ ion–irradiated Ti_3SiC_2 sample, some voids with a diameter of 10–30 nm associated with dislocations were also observed in the irradiated region, as displayed in Figure 3A–C. These faceted voids with a hexagonal shape are surrounded with dislocations, vacancies, interstitials, and possibly amorphous, as shown in Figure 3C. It has been reported that the MAX phases were not stable and could decompose under radiation environments accompanying with the out-diffusion of the A atoms and the formation of voids and MX precipitates.[16] Needle-like precipitates were observed in the neutron-irradiated Ti_2AlC with the damage up to 10 dpa.[21] Al atoms were found to be sputtered away from the Ti_3AlC_2 sample under an electron beam irradiation.[37] A TiC nanocrystalline phase was formed in Ti_3SiC_2 under the 2 MeV iodine ion irradiation.[31] However, different from these researches, no obvious secondary phases, such as TiC and/or SiC, have been observed in this Ti_3SiC_2 sample. Compared to the unirradiated region, the EDS mapping results indicate that the content of Si and Ti in the irradiation-induced voids region was obviously reduced, as shown in Figure 3D–I. However, the EDS elemental composition ratio results in Figure 4 illustrate that the atomic ratios of Ti and Si are both approximately equal to 3:1 in the unirradiated and irradiated regions, including the void area, which is consistent with the atomic stoichiometry of Ti_3SiC_2. This result indicates that the formation of these voids was not due to the decomposition of Ti_3SiC_2 phase in this Si^+ ion–irradiated Ti_3SiC_2 sample.

In addition, some related researches reported that cavities/voids in the Ti_3SiC_2 were observed only along GBs or near the TiC particles, whereas in the Ti_2AlC, small cavities were observed throughout the matrix phase after irradiation.[21,22] As shown in Figure 3A, no secondary phase can be observed in this Ti_3SiC_2 sample and most of the radiation-induced voids are attached to the dislocations, not the pristine GBs. It is also worth emphasizing that most of the dislocations were formed by the Si^+ ion irradiation as the density of dislocations in the unirradiated region is very small. The ion irradiation–induced interstitial atoms can be aggregated to form dislocations. The voids/cavities can be formed by the aggregation of vacancies.[38] Thus, the formation of these voids/cavities was due to the absorption of vacancies by the dislocations that formed during the ion irradiation process. As the present irradiation temperature (300°C) was not high, neither the interstitial atoms nor the vacancies could move for a long distance to the GB. Therefore, these voids were just right attached to the dislocations.

After being annealed at 900°C for 5 h, a band centered to the peak damage region with much visible voids/cavities can be seen in the irradiated sample, as shown in Figure 4A. The sizes of the voids/cavities at the GBs are much larger over those inside the grains, which was due to the trapping effect of the GBs.[35] In addition to the formation of a large number of voids/cavities, some SFs were also observed in the annealed sample with two of them indicated by arrows in Figure 4A. As indicated by the SAED pattern in Figure 4A, the irradiated region with an FCC structure was found to have transformed back to its original HCP structure after annealing. The HRTEM image in Figure 5B shows that there is still a small amount

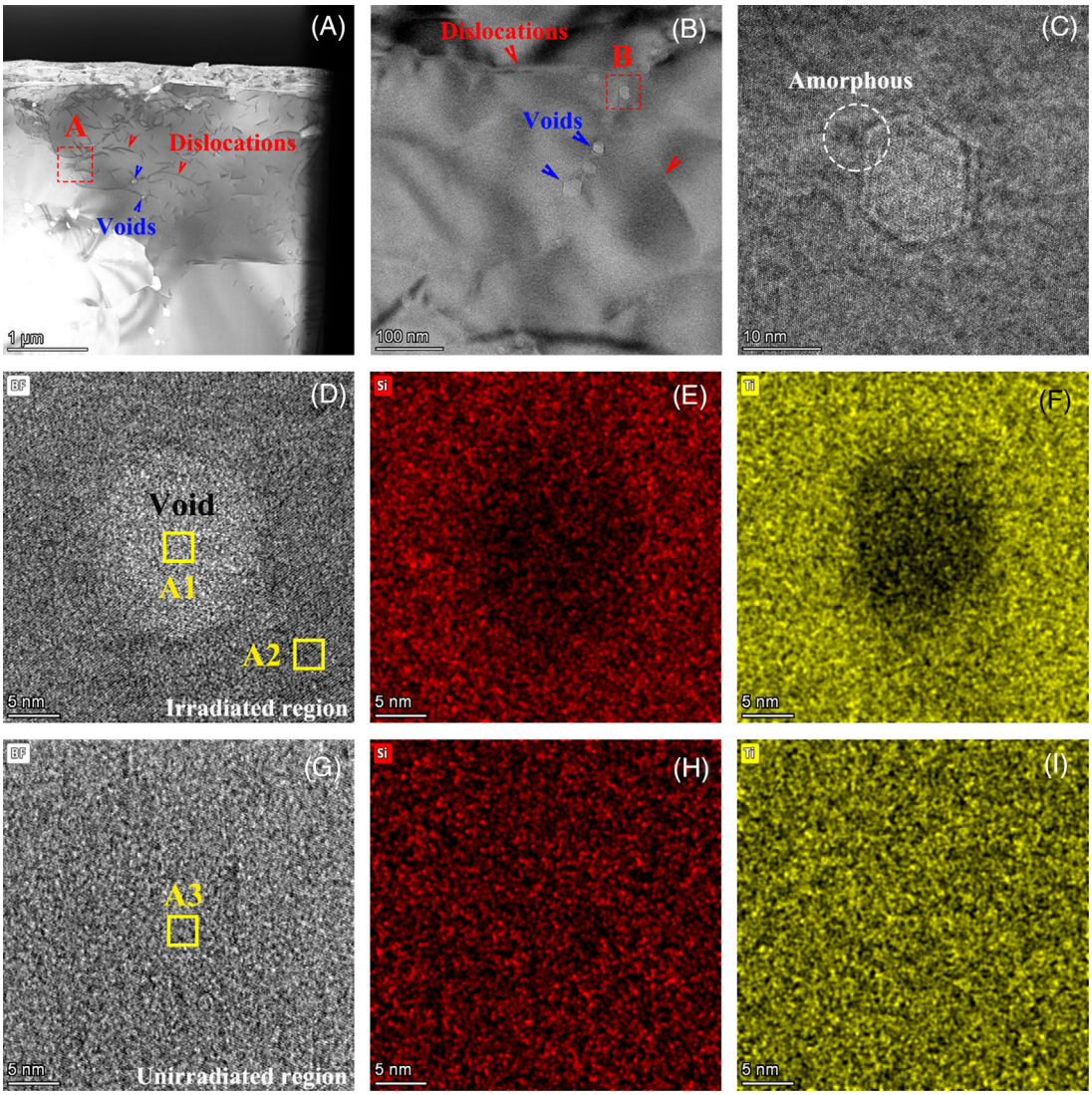

FIGURE 3 (A) An X-STEM image of the Si^+ ion–irradiated region in Ti_3SiC_2 sample; (B) a magnified image of the "A" region in (A); (C) a magnified image of the "B" region in (B); (D) a bright-field HAADF STEM image of the irradiated region in a Ti_3SiC_2 sample; (E) and (F) are the Si and Ti EDS mapping results of (D), respectively; (G) a bright-field HAADF STEM image of the unirradiated region in a Ti_3SiC_2 sample; (H) and (I) are the Si and Ti EDS mapping results of (G), respectively. EDS, energy-dispersive spectroscopy

of amorphous area in the irradiated area after annealing. The shape of the cavities/voids has changed from the hexagonal to rectangular shapes. The average size of the cavities/voids inside the crystal grains is about 20 nm. Density functional theory simulation results[39] have indicated that the radiation-induced C, Si, and Ti interstitials tend to rapidly migrate through the Si layers before being captured or annihilated. On the other hand, the Si vacancy with the migration energy of 0.61 eV is mobile at high temperatures, whereas C and Ti vacancies with the migration energies of 4.13 and 3.51 eV, respectively, are not. Thus, cavities/voids are mainly distributed in the peak damage region, whereas the dislocations and SFs are widely distributed throughout the whole irradiation region. These results agree with our observations in the annealed sample. Actually, the evolution of defects is affected by complex factors, among which temperature is one of the most important factors. The T/T_M (homologous irradiation temperature, where the T_M is the melting point) has been widely used to categorize the temperature dependence of radiation response.[40,41] The amorphization of a crystal structure, the migration of interstitials, the migration of monovacancy, and the migration of vacancy-clusters processes are corresponding to four temperature ranges from I to IV in irradiated materials. The formation process of void/cavity in irradiated materials locates at the III temperature range, and the 900°C annealing process for the Si^+ ion–irradiated Ti_3SiC_2 sample in this work is in this temperature range.

In the Si^+ ion irradiated and annealed Ti_3SiC_2 sample, ripplocation (RP) structures were observed in the irradiated region but not in the unirradiated regions. Some of the RPs are marked by white arrows in the Figure 5C.

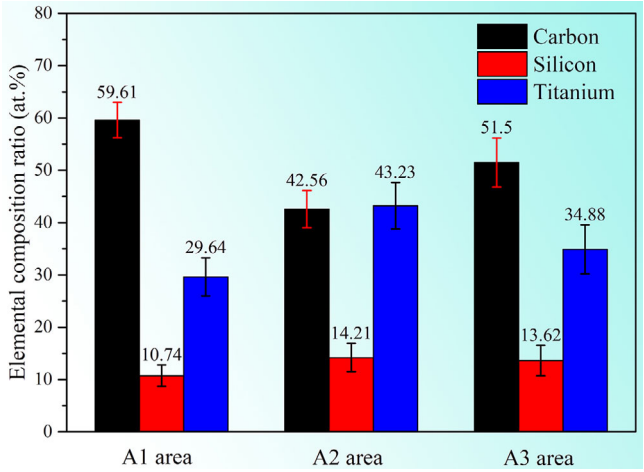

FIGURE 4 The EDS elemental composition ratio results of the three areas that marked by yellow squares in Figure 3D,G. EDS, energy-dispersive spectroscopy

Two groups of RPs with different orientations formed a boundary, which is marked by a white dashed curve in Figure 5C. "RP" is a line defect first observed and termed by Kushima et al., and its formation mechanisms are shown in Figure 5D.[42] The self-energy of an RP is sublinearly related with the value of its burgers vector, which makes the same-sign RPs tend to merge. These kinds of RPs have been observed in pristine MAX phases resulted from growth defects or induced by deformation.[31] However, under the ion irradiation and high-temperature annealing conditions, the volumetric swelling can generate the compressive stress inside the material. Meanwhile, Si atoms undergo a recrystallization reaction with the irradiation-induced C and/or Ti interstitial atoms, which introduces additional structural units into some local regions. These two situations can synergistically result in the formation of RPs during the ion irradiation and annealing processes.

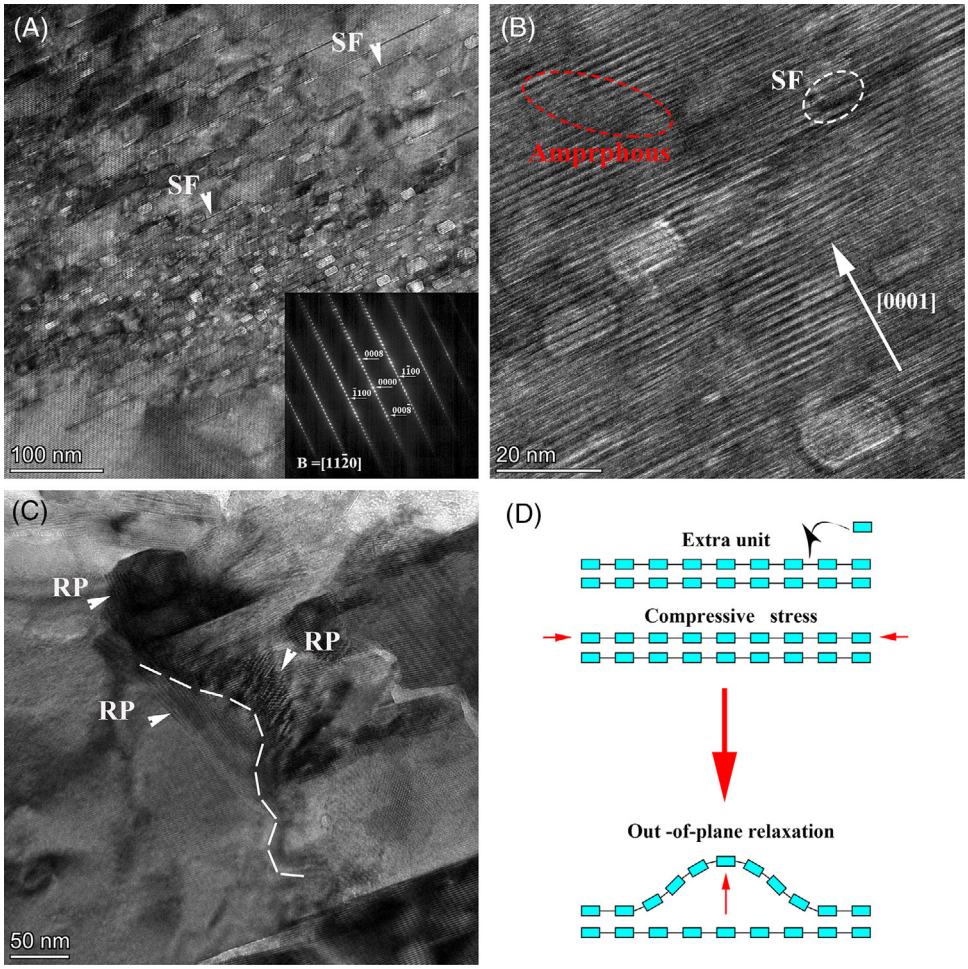

FIGURE 5 X-TEM BF images of the irradiated and annealed Ti_3SiC_2 sample: (A) the image of the peak damage region and its corresponding SAED pattern in the inset; (B) a magnified HRTEM image from the center of (A); (C) a BF image showing the irradiated region with ripplocations; and (D) schematic drawing showing the formation mechanisms of ripplocations. BF, bright-field; HRTEM, high-resolution TEM; SAED, selected area electron diffraction

4 | CONCLUSIONS

The main conclusions of the microstructure evolutions of the Si^+ ion–irradiated and annealed Ti_3SiC_2 samples are listed as follows:

1. Ti_3SiC_2 was found to have transformed from its HCP structure into an FCC structure after irradiation without any secondary phases formed. Some hexagonal voids/cavities were formed in the irradiated Ti_3SiC_2, which was due to the absorption of vacancies by the dislocations.
2. Some HSDNs and SFs were formed at the boundaries between the irradiated and unirradiated regions. The hexagonal dislocation networks are the products of dislocations reactions. In the crystalline of an FCC structure, it can be transformed from the rectangular dislocation networks. In the crystal of an HCP structure, it can be formed by the decomposition reaction of perfect dislocations with the formation of SFs.
3. After annealing treatment, the irradiated Ti_3SiC_2 has transformed its structure from FCC back to HCP. High-density cavities were generated at the damage peak region. Due to the difference in migration energy of vacancies and interstitial atoms, cavities are mainly distributed in the peak damage region, whereas the dislocations and SFs are widely distributed throughout the whole irradiation area after annealing. These grouped defects were formed along the basal planes.
4. After annealing, RPs have been observed in the irradiated region in Ti_3SiC_2 samples but not the unirradiated region. In addition to the possibility that RPs were formed in the original sample during the preparation process, compressive stress induced by the volumetric swelling during the ion irradiation process and extra structural units that introduced into the irradiated Ti_3SiC_2 during the high-temperature annealing process are also the reasons for its formation.

Our experimental results of microstructure evaluation and insights into the formation processes and corresponding mechanisms of these defect structures might benefit the design of advanced irradiation tolerance materials in next generation reactors.

ACKNOWLEDGMENT

The work was supported by NPL, CAEP, through Project 2015AB001 and National major scientific research equipment development of China, through Grant No. 11227804. Q. P. would like to acknowledge the support provided by LiYing Program of the Institute of Mechanics, Chinese Academy of Sciences through Grant No. E1Z1011001.

ORCID

Chao Ye https://orcid.org/0000-0001-6841-8647

REFERENCES

1. Zhou XB, Han YH, Shen XF, Du SY, Lee J, Huang Q. Fast joining SiC ceramics with Ti_3SiC_2 tape film by electric field-assisted sintering technology. J Nucl Mater. 2015;466:322–7.
2. Tatarko P, Casalegno V, Hu CF, Salvo M, Ferraris M, Reece MJ. Joining of CVD-SiC coated and uncoated fibre reinforced ceramic matrix composites with pre-sintered Ti_3SiC_2 MAX phase using spark plasma sintering. J Eur Ceram Soc. 2016;36(16):3957–67.
3. Medvedeva NI, Enyashin AN, Ivanovsky AL. Modeling of the electronic structure, chemical bonding, and properties of ternary silicon carbide Ti_3SiC_2. J Struct Chem. 2011;52(4):806–22.
4. Istomin PV, Nadutkin AV, YuI Ryabkov, Goldin BA. Preparation of Ti_3SiC_2. Inorg Mater. 2006;42:250–5.
5. Zhang ZF, Sun ZM, Hashimoto H. Deformation and fracture behavior of ternary compound Ti_3SiC_2 at 25-1300°C. J Mater Lett. 2003;57:1295–9.
6. Barsoum MW, El-Raghy T. Processing and mechanical properties of Ti_3SiC_2: reaction path and microstructure evolution. J Am Ceram Soc. 1999;82:2849–54.
7. Perevislov SN, Sokolova TV, Stolyarova VL. The Ti_3SiC_2 max phases as promising materials for high temperature applications: formation under various synthesis conditions. Mater Chem Phys. 2021;267:124625.
8. Qi Q, Cheng GJ, Shi LQ, O'Connor DJ, King BV, Kisi EH. Damage accumulation and recovery in C^+-irradiated Ti_3SiC_2. Acta Mater. 2014;66:317–25.
9. Sun ZM. Progress in research and development on MAX phases: a family of layered ternary compounds. Int Mater Rev. 2011;56(3):143–66.
10. Sokol M, Natu V, Kota S, Barsoum MW. On the chemical diversity of the MAX phases. Trends Chem. 2019;1(21):210–23.
11. Hoffman EN, Vinson DW, Sindelar RL, Tallman DJ, Kohse G, Barsoum MW. MAX phase carbides and nitrides: properties for future nuclear power plant in-core applications and neutron transmutation analysis. Nucl Eng Des. 2012;244:17–24.
12. Wang ZY, Ma GS, Li ZC, Ruan HT, Yuan JH, Wang L, et al. Corrosion mechanism of Ti_2AlC MAX phase coatings under the synergistic effects of water vapor and solid NaCl at 600°C. Corr Sci. 2021;192:109788.
13. Barnes LA, Dietz Rago NL, Leibowitz L. Corrosion of ternary carbides by molten lead. J Nucl Mater. 2008;373(1–3):424–8.
14. Xie J, Wang XH, Li AJ, Li FZ, Zhou YC. Corrosion behavior of selected $M_{n+1}AX_n$ phases in hot concentrated HCl solution: effect of A element and MX layer. Corros Sci. 2012;60:129–35.
15. Wang CX, Yang TF, Tracy CL, Lu C, Zhang H, Hu YJ, et al. Disorder in $M_{n+1}AX_n$ phases at the atomic scale. Nat Commun. 2019;10:622.
16. Wang CX, Tracy CL, Ewing RC. Radiation effects in $M_{n+1}AX_n$ phases. Appl Phys Rev. 2020;7:041311.
17. Tallman DJ, Hoffman EN, Caspi EN, Kohse G, Sindelar RL, Barsoum MW, et al. Effect of neutron irradiation on select MAX phases. Acta Mater. 2015;85:132–43.

18. Tallman DJ, He L, Garcia-Diaz BL, Hoffman EN, Kohse G, Sindelar RL, et al. Effect of neutron irradiation on defect evolution in Ti_3SiC_2 and Ti_2AlC. J Nucl Mater. 2016;468:194–206.
19. Filbert DI, Travitzky N, Motz G, Zhitomirsky I, Greil P. Polymer derived ceramics reinforced with Ti_3SiC_2 coated SiC fibers: a feasibility study. Mater Lett. 2015;145:229–31.
20. Spencer CB, Córdoba JM, Obando NH, Radovic M, Odén M, Hultman L, et al. The reactivity of Ti_2AlC and Ti_3SiC_2 with SiC fibers and powders up to temperatures of 1550°C. J Am Ceram Soc. 2011;94(6):1737–43.
21. Tunes MA, Harrison RW, Donnelly SE, Edmondson PD. A transmission electron microscopy study of the neutron-irradiation response of Ti-based MAX phases at high temperatures. Acta Mater. 2019;169:237–47.
22. Tallman DJ, He LF, Gan J, Caspi EN, Hoffman EN, Barsoum M.W., Effects of neutron irradiation of Ti_3SiC_2 and Ti_3AlC_2 in the 121-1085°C temperature range. J Nucl Mater. 2017;484:120–34.
23. Zhang H, Hu T, Wang XH, Zhou YC. Structural defects in Max phases and their derivative Mxenes: a look forward. J Mater Sci Technol. 2020;38:205–20.
24. Song P, Sun J, Wang Z, Cui M, Shen T, Li Y, et al. Irradiation resistance properties studies on helium ions irradiated MAX phase Ti_3AlC_2. Nucl Instrum Methods Phys Res Sect B-Beam Interact Mater Atoms. 2014;326:332–6.
25. Whittle KR, Blackford MG, Aughterson RD, Moricca S, Lumpkin GR, Riley DP, et al. Radiation tolerance of Mn+1AXn phases, $Ti3AlC_2$ and Ti_3SiC_2. Acta Mater. 2010;58:4362–8.
26. Wang CX, Yang TF, Xiao JR, Liu S, Xue J, Huang Q, et al. Structural transitions induced by ion irradiation in V_2AlC and Cr_2AlC. J Am Ceram Soc. 2016;99:1769–77.
27. Nappe JC, Maurice C, Grosseau P, Audubert F, Thomé L, Guilhot B, et al. Microstructural changes induced by low energy heavy ion irradiation in titanium silicon carbide. J Eur Ceram Soc. 2011;31:1503–11.
28. Clark DW, Zinkle SJ, Patel MK, Parish CM. High temperature ion irradiation effects in MAX phase ceramics. Acta Mater. 2016;105:130–46.
29. Zhang HL, Su RR, Szlufarskab I, Shi LQ, Wen HM. Helium effects and bubbles formation in irradiated Ti_3SiC_2. J Eur Ceram Soc. 2021;41:252–8.
30. Liu SS, Yang TF, Zhang J, Yan Z, Lu Y, Han D, et al. Thermal effects in ion irradiated Ti_2AlC and Ti_3SiC_2. Nucl Instrum Methods Phys Res B. 2018;435:50–5.
31. Zhang L, Qi Q, Shi LQ, O'Connor DJ, King BV, Kisi EH, et al. Damage tolerance of Ti_3SiC_2 to high energy iodine irradiation. Appl Surf Sci. 2012;258:6281–7.
32. Hantcherli M, Pettinari-Sturmel F, Viguier B, Douin J, Coujou A. Evolution of interfacial dislocation network during anisothermal high-temperature creep of a nickel-based superalloy. Scr Mater. 2012;66:143–6.
33. Xie J, Tian SG, Shang LJ, Zhou XM. Creep behaviors and role of dislocation network in a powder metallurgy Ni-based superalloy during medium-temperature. Mater Sci Eng A. 2014;606:304–12.
34. Gao Q, Liu LR, Tang XH, Peng ZJ, Zhang MJ, Tian SG. Evolution of interfacial dislocation networks during long term thermal aging in Ni-based single crystal superalloy DD5. China Foundry. 2019;16(1):14–22
35. Kamaraj M, Mayr C, Kolbe M, Eggeler G. On the influence of stress state on rafting in the single crystal superalloy CMSX-6 under conditions of high temperature and low stress creep. Scr Mater. 1998; 38(4):589–94.
36. Hull D, Bacon DJ. Introduction to dislocations. Oxford: Elsevier Ltd.; 2011.
37. Huang XC, Feng Y, Dou YK, Tang H, Ding DD, Tian P, et al. Effect of electron irradiation on Ti_3AlC_2. Scr Mater. 2016;113:114–7.
38. Lu C, Niu L, Chen N, Jin K, Yang T, Xiu P, et al. Enhancing radiation tolerance by controlling defect mobility and migration pathways in multicomponent single phase alloys. Nat Commun. 2016;7:13564.
39. Middleburgh SC, Lumpkin GR, Riley D. Accommodation, accumulation, and migration of defects in Ti_3SiC_2 and Ti_3AlC_2 max phases. J Am Ceram Soc. 2013;96(10):3196–201.
40. Zinkle SJ, Blanchard JP, Callis RW, Kessel CE, Kurtz RJ, Lee PJ, et al. Fusion materials science and technology research opportunities now and during the ITER era. Fusion Eng Des. 2014;89(7–8):1579–85.
41. Zinkle SJ, Busby JT. Structural materials for fission & fusion energy. Mater Today. 2009;12(11):12–9.
42. Kushima A, Qian XF, Zhao P, Zhang SL, Li J. Ripplocations in van der waals layers. Nano Lett. 2015;15:1302–8.

How to cite this article: Ye C, Chang Q, Lei P, Dong W, Peng Q. Microstructure evolution in Si^+ ion irradiated and annealed Ti_3SiC_2 MAX phase. J Am Ceram Soc. 2022;105:5921–5928. https://doi.org/10.1111/jace.18510